the M^I hydrate.[45] Neutron diffraction and ^1H NMR studies place the oxygen in the plane of the alkali-metal layer with the two hydrogen atoms directed toward the sulfur layers in the monohydrates and toward another H_2O in the same plane and a sulfur layer in the bilayer.[21]

The most striking similarity between the hydration behavior of the intercalated disulfides and 2H-, 3R-K_xYClO and 3R-Rb_xYClO is the similarity of Δc in the latter, ~2.6 Å (Table II), and the evident trigonal-prismatic coordination of M^I (Figure 5). On this basis, we can probably conclude that the present phases also contain a monolayer of H_2O in trigonal-prismatic sites with the hydrogen atoms near the Cl layers. As with the hydrated dichalcogenides, the hydration-dehydration (3R-1T or 2H-2H) reactions of the chloride are reversible with the original YOCl phase being obtained on dehydration.

In the case of 3R-Li_xYClO, there is no hydration reaction in air, in contrast with Li_xMS_2 which forms bilayer hydrates, perhaps because the lattice energy with a more polar substrate is higher than the Li^+ hydration energy. The lithium salt was studied only at relatively low humidities, although liquid water was also without effect, while the behavior of the sodium compound was not investigated.

When the phases 3R-M^I_xYClO, M = Li-Cs and $x \simeq 0.1$-0.2, are placed in water, they are oxidized, as evidenced by the evolution of gas, and the crystals exfoliate. The $M^I_xMS_2$ phases for group 4 and 5 transition metals are evidently weaker reducing agents as they generally form crystalline hydrates and only reduce liquid water for x greater than 0.3-0.6.[46] When hydrogen is intercalated electrolytically into single crystals of 2H-TaS_2 in dilute acid, there is a large degree of exfoliation with no gas evolution.[47] The exfoliation in both cases is similar in appearance to the swelling observed in smectites or vermiculites and in particular the alkali-metal montmorillonites, $\sim M^I_x(Al,Mg)_4Si_8O_{20}(OH)_4 \cdot nH_2O$,[48] where the hydration is dominated by hydrogen bonding to the oxygen layers.

A "mechanism" for the exfoliation of 3R-M^I_xYClO may be postulated on the basis of visual evidence and the results for other systems. The first step is the hydration of M^I to form 1T-$M^I_x(H_2O)_aYClO$. This is followed by the oxidation of the slabs with loss of M^IOH and H_2 to give neutral (or lower charged) YClO slabs, perhaps with some decomposition. Some remaining water is hydrogen bonded to the chlorine layers. It is further hydration and hydrogen bonding within the interlayer region that causes the swelling or exfoliation. When these exfoliated "crystals" are removed from the water and mildly heated, most of the water evaporates and the "crystals" collapse back to plates. The plates must retain some water to allow the process to be repeatedly reversed, since the exfoliation cannot be repeated after the exfoliated "crystals" are dehydrated by heating. The phase at this point gives only very broad diffraction lines. In contrast, the 2H-M^I_xYClO phases, M = K or Rb, apparently form monolayer hydrates on exposure to moisture with no structural change as there are already TP sites available for H_2O. These 2H-type hydrates did not exfoliate or evolve H_2 in water.

The related 1T carbides, $M^I_xY_2Cl_2C$ with $x \simeq 1$ and M = Li, K, and Cs, have all been prepared, and the crystal structure confirmed with a single-crystal study of the potassium derivative. Both M^I and C occur in all TAP sites. These compounds decompose in moist air or water.[17] Intercalation of the analogous zirconium carbide phase has been unsuccessful, as is also true for the zirconium halide oxide and hydride analogues.

Acknowledgment. The authors are indebted to Prof. R. A. Jacobson and his group for continued X ray crystallographic services and to F. C. Laabs for the microprobe analyses.

Registry No. YClO, 13759-29-0; Y, 7440-65-5; Y_2O_3, 1314-36-9; NaCl, 7647-14-5; KCl, 7447-40-7; LiCl, 7447-41-8; CsCl, 7647-17-8; RbCl, 7791-11-9; sodium yttrium chloride oxide, 86993-42-2; potassium yttrium chloride oxide, 86993-37-5; lithium yttrium chloride oxide, 86993-32-0; cesium yttrium chloride oxide, 86993-29-5; rubidium yttrium chloride oxide, 86993-39-7.

Supplementary Material Available: Tables of the observed and calculated structure factor data for 2H-$K_{0.08}YClO$ and 3R-$Na_{0.08}YClO$ and the observed and calculated powder patterns for 1T-Cs_xYClO and 1T-$K_x(H_2O)_aYClO$ (4 pages). Ordering information is given on any current masthead page.

(45) Bos-Albernick, A. J. A.; Haange, R. J.; Wiegers, G. A. *J. Less-Common Met.* **1979**, *63*, 69.
(46) Schöllhorn, R. In "Intercalation Chemistry"; Whittingham, M. S., Jacobson, A. J., Eds., Academic Press: New York, 1982; p 324.
(47) Murphy, D. W.; Hull, C. W. *J. Chem. Phys.* **1975**, *62*, 973.
(48) Grim, R. F. "Clay Mineralogy"; McGraw-Hill: New York, 1968.

Contribution from the Department of Chemistry, Gorlaeus Laboratories, State University Leiden, 2300 RA Leiden, The Netherlands

Magnetic Properties of Dimeric Disubstituted-Triazole Copper(II) Compounds. X-ray Structure of Bis[μ-3,5-bis(pyridin-2-yl)-1,2,4-triazolato-N',N^1,N^2,N']-bis[aqua(trifluoromethanesulfonato-O)copper(II)]

ROB PRINS, PAUL J. M. W. L. BIRKER, JAAP G. HAASNOOT,* GERRIT C. VERSCHOOR, and JAN REEDIJK

Received February 13, 1985

The crystal and molecular structure of bis[μ-3,5-bis(pyridin-2-yl)-1,2,4-triazolato-N',N^1,N^2,N']bis[aqua(trifluoromethanesulfonato-O)copper(II)] ($[Cu(bpt)(CF_3SO_3)(H_2O)]_2$, bpt = $C_{12}N_5H_8^-$) was determined by X-ray diffraction methods. Crystal data: triclinic, centrosymmetric, space group $P\bar{1}$ with a = 8.841 (3) Å, b = 14.131 (6) Å, c = 14.392 (6) Å, α = 112.58 (3)°, β = 92.23 (3)°, γ = 102.45 (3)°, Z = 2, and V = 1606 (1) Å^3. The least-squares refinement based on 2832 significant reflections converged at R = 0.023 and R_w = 0.025. The structure consists of dimeric units $[Cu_2L_2]^{2+}$ with a copper-copper distance of 4.085 (1) Å. Each symmetry-independent CuN_4O_2 chromophore in the dimer is a six-coordinate distorted octahedron. The oxygen donor ligands are a water molecule and a triflate anion. The Cu atoms in the dimer are bridged by two triazole rings. The magnetic susceptibility measurements show quite large antiferromagnetic interactions with a singlet-triplet splitting of 204-236 cm^{-1} between the metal centers in a series of isostructural copper(II) compounds with the anions NO_3^-, ClO_4^-, BF_4^-, and $CF_3SO_3^-$. Strong magnetic interactions in these compounds having a singlet ground state was also evident from the temperature dependence of the intensity of the excited triplet state as observed in powder EPR spectra. In addition the powder EPR spectrum of the title compound revealed copper hyperfine interactions at 77 K.

Introduction

The magnetic properties of paramagnetic transition-metal ions incorporated in various coordination compounds have been the subject of intensive study over the past decades. The best known examples are dinuclear copper(II) compounds. Useful correlations between the singlet-triplet splitting, which is mainly determined by the exchange interaction between ground-state magnetic orbitals, and structural parameters have been made.[1-3] Another

(1) Hodgson, D. J. *Prog. Inorg. Chem.* **1975**, *19*, 173.

0020-1669/85/1324-4128$01.50/0

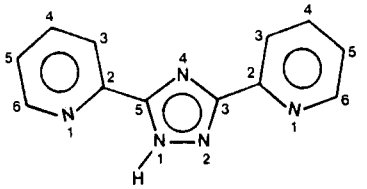

Figure 1. Structural formula and numbering system of 3,5-bis(pyridin-2-yl)-1*H*-triazole (bptH).

Table I. Copper Compounds with bpt

compd no.	formula	color	% metal calcd	% metal found
1	$Cu_2(bpt)_2(CF_3SO_3)_2(H_2O)_2$	blue	14.0	13.9
2	$Cu_2(bpt)_2(ClO_4)_2(H_2O)_4$	blue	15.1	14.9
3	$Cu_2(bpt)_2(NO_3)_2(H_2O)_{2.5}$	blue	17.0	16.8
4	$Cu_2(bpt)_2(BF_4)(H_2O)_3$	blue	15.9	15.6

interesting aspect of these compounds is their potential use as models for biological dimetallic sites.[4-7] These are the two major reasons that these compounds are receiving relatively much attention. To investigate the magnetic and spectroscopic properties of triazole-bridged dinuclear copper compounds, we selected the ligand 3,5-bis(pyridin-2-yl)-1,2,4-triazole (Figure 1), hereafter abbreviated as bptH. 1,2,4-Triazole derivatives are a class of azole compounds that can act as either 2,4- or 1,2-bridging nitrogen donor ligands.[8-13] Because the 1,2-bridging mode is known to yield polynuclear coordination compounds,[9-13] it seemed appropriate to incorporate this mode in a chelating ligand. Although Geldard and Lions,[14] who first synthesized bptH, expected the ligand to be a terdentate analogue of terpyridine, it seemed equally possible and perhaps even more likely that both pyridine nitrogen atoms would be directed toward the triazole N1 and N2, making this dinucleating configuration more favorable than the terdentate one. In this mode bptH is closely related to ligands such as 3,5-bis(pyridin-2-yl)-4-amino-1,2,4-triazole and 1,4-dihydrophthalazine, with which dinuclear coordination compounds are known to be formed.[15-17]

The series of isostructural copper compounds discussed in the present paper involves bpt as a deprotonated anionic ligand whose configuration is related to that of the perchlorate salt[18] of $(bptH_2)^+$. The structure of the copper(II) triflate compound with bpt, as well as the spectroscopic and magnetic properties of the whole series of copper(II) bpt compounds with $CF_3SO_3^-$, NO_3^-, ClO_4^-, and BF_4^- as anions will be described.

Experimental Section

Starting Materials. Commercially available solvents and hydrated metal salts were used without further purification. The ligand bptH was synthesized according to the method of Geldard and Lions,[14] with use of 2-cyanopyridine obtained from Fluka A.G. and hydrazine hydrate obtained from Janssen Chimica as starting materials.

Synthesis of the Coordination Compounds. All complexes were prepared by mixing 4 mmol of the metal salt, dissolved in 20 mL of hot water with 30 mL of a hot methanolic solution containing 2 mmol of bpt. The solutions were concentrated, filtered, and left to stand at ambient temperature. The dark blue crystals or powders that separated from the solution were filtered, washed with water, and dried in air. The resulting compounds are listed in Table I.

Characterization. IR spectra in the 4000–180-cm^{-1} region were recorded on a Perkin-Elmer 580B spectrophotometer as both Nujol mulls and CsCl pellets. The infrared spectra of the above-mentioned compounds were all very similar with respect to the band positions and the relative intensities of the ligand vibrations, from which similar structures were concluded. No attempt was made to interpret the mode of coordination of the anions from their IR absorption bands, since misinterpretation is likely to occur due to the participation of these anions in hydrogen bridges.

Electronic spectra in the region 28 000–4000 cm^{-1} were recorded on a Perkin-Elmer 330 spectrophotometer using the diffuse-reflectance method with MgO as a reference.

Cu, C, N, and H analyses were carried out by the Pascher Analytical Laboratory, Bonn, West Germany, and the Microanalytical Laboratory of the University College Dublin, Dublin, Ireland.

Magnetic Measurements. Magnetic susceptibility data in the temperature region 80–300 K were obtained on powdered samples with an automated Faraday balance. The observed susceptibilities, corrected for temperature-independent paramagnetism and diamagnetism (using Pascal constants) were fitted to the theoretical expression for the susceptibility by means of least-squares methods. Details of the Faraday setup have been described by Arbouw.[19]

EPR spectra of the powdered compounds were recorded at room and liquid-nitrogen temperatures with a Varian E-3 spectrometer operating at X-band frequencies (9 GHz).

Collection and Reduction of X-ray Intensity Data. A crystal of the related compound $[Cu(bpt)(NO_3)(H_2O)]_2(H_2O)_{0.5}$ was initially selected to determine the structure. The triclinic unit cell with cell parameters a = 9.443 (2) Å, b = 57.134 Å, c = 10.94 (1) Å, α = 90.26 (1)°, β = 108.32 (8)°, γ = 89.86 (1)°, V = 5106 Å^3, and Z = 8 (dimeric units) showed a tendency toward pseudomonoclinic behavior. With use of the 5146 significant reflections the structure could be refined to values of R = 0.10 and R_w = 0.113. Due to high correlations between the atomic parameters no further progress in the refinement could be made. However, the structure of the dinuclear units was essentially the same as the one described in detail in this paper.

Subsequently a bar-shaped single crystal of the title compound $[Cu(bpt)(CF_3SO_3)(H_2O)]_2$ (**1**) was obtained that appeared to be suitable for a detailed structure determination. Diffraction data were measured at room temperature, with an Enraf-Nonius CAD-4 automatic four-circle diffractometer (graphite-monochromated Mo Kα radiation; $\lambda(\alpha_1)$ =

Table II. Summary of Crystal Data and Intensity Collection of **1**

formula	$[Cu(C_{12}N_5H_8)(CF_3SO_3)(H_2O)]_2$
mol wt	905.70
space group	$P\bar{1}$
a, Å	8.841 (3)
b, Å	14.132 (6)
c, Å	14.392 (6)
α, deg	112.58 (3)
β, deg	92.23 (3)
γ, deg	102.45 (3)
V, Å^3	1606 (1)
Z	2 (dimers)
D_{obsd} (by flotation), Mg m^{-3}	1.85 (2)
D_{calcd}, Mg m^{-3}	1.87
cryst size, mm^3	0.5 × 0.05 × 0.05
μ(Mo Kα), cm^{-1}	15.51
θ range, deg	2–22
data collection range	h, −9 to +9; k, −14 to +14; l, −15 to +15
no. of indep reflecns	3923
no. of signif reflecns ($I > 2\sigma(I)$)	2832
F(000)	909.74
final R (R_w)	0.023 (0.025)

(2) Crawford, V. H.; Richardson, H. W.; Wasson, J. R.; Hodgson, D. J.; Hatfield, W. E. *Inorg. Chem.* **1976**, *15*, 2107 and references therein.
(3) Hatfield, W. E. *ACS Symp. Ser.* **1975**, *No. 5*, 108.
(4) Kolks, G.; Lippard, S. J.; Waszczak, J. V.; Lilienthal, H. R. *J. Am. Chem. Soc.* **1982**, *104*, 717.
(5) Fee, J. A. *Struct. Bonding (Berlin)* **1975**, *23*, 1.
(6) Solomon, E. I. *Met. Ions Biol.* **1981**, *3*, 41.
(7) Ibers, J. A.; Holmes, R. H. *Science (Washington, D.C.)* **1980**, *209*, 223.
(8) Engelfriet, D. W. Ph.D. Thesis, State University Leiden, 1979. Engelfriet, D. W.; Groeneveld, W. L.; Groenendijk, H. A.; Smit, J. J.; Nap, G. M. *Z. Naturforsch., A* **1980**, *35A*, 115.
(9) Inoue, M.; Kubo, M. *Coord. Chem. Rev.* **1976**, *21*, 1.
(10) Jarvis, J. A. *Acta Crystallogr.* **1962**, *15*, 964.
(11) Reimann, C. W.; Zocchi, M. *Acta Crystallogr., Sect. B: Struct. Crystallogr. Cryst. Chem.* **1971**, *B27*, 682.
(12) Vos, G. Ph.D. Thesis, State University Leiden, 1983. Vos, G.; le Febre, R. A.; de Graaff, R. A. G.; Haasnoot, J. G.; Reedijk, J. *J. Am. Chem. Soc.* **1983**, *105*, 1682.
(13) van Albada, G. A.; de Graaff, R. A. G.; Haasnoot, J. G.; Reedijk, J. *Inorg. Chem.* **1984**, *23*, 1404.
(14) Geldard, J. F.; Lions, F. *J. Org. Chem.* **1965**, *30*, 318.
(15) Keij, F. S.; de Graaff, R. A. G.; Haasnoot, J. G.; Reedijk, J. *J. Chem. Soc., Dalton Trans.* **1984**, 2093.
(16) Andrew, J. E.; Blake, A. B. *J. Chem. Soc. A* **1969**, 1408.
(17) Banci, L.; Bencini, G.; Benelli, C.; Gatteschi, D. *Inorg. Chem.* **1982**, *21*, 3868.
(18) Prins, R.; Birker, P. J. M. W. L.; Verschoor, G. C. *Acta Crystallogr., Sect. B: Struct. Crystallogr. Cryst. Chem.* **1982**, *B38*, 2934.
(19) Arbouw, J. W. Ph.D. Thesis, State University Leiden, 1974.

Table III. Atomic Fractional Coordinates ($\times 10^5$ for Cu; $\times 10^4$ for C, N, O, S, and F) and Isotropic Thermal Parameters ($\times 10^3$ Å^2 for Cu; $\times 10^2$ Å^2 for C, N, O, S, and F; $B_{iso} = {}^8/_3\pi^2$ trace (U)) of $[Cu(bpt)(CF_3SO_3)(H_2O)]_2$ (**1**) (for Non-Hydrogen Atoms)[a]

atom	x/a	y/b	z/c	B(iso)
Cu(1)	−10320 (6)	−17722 (4)	19115 (3)	2344 (15)
Cu(2)	18144 (6)	−30358 (4)	31437 (3)	2352 (15)
N(11)	495 (3)	−1221 (2)	3118 (2)	229 (9)
N(12)	1393 (3)	−1644 (2)	3546 (2)	229 (9)
N(14)	1744 (3)	52 (2)	4589 (2)	203 (8)
C(13)	2116 (4)	−874 (3)	4405 (3)	199 (10)
C(15)	726 (4)	−214 (3)	3760 (3)	199 (10)
N(151)	−1088 (3)	−187 (2)	2524 (2)	215 (8)
C(152)	−132 (4)	396 (3)	3419 (3)	202 (10)
C(153)	62 (5)	1465 (3)	3906 (3)	262 (12)
C(154)	−711 (5)	1985 (3)	3484 (3)	312 (13)
C(155)	−1648 (5)	1415 (3)	2581 (3)	310 (13)
C(156)	−1803 (5)	341 (3)	2130 (3)	277 (12)
N(131)	3273 (3)	−2189 (2)	4528 (2)	209 (9)
C(132)	3200 (4)	−1158 (3)	4987 (3)	202 (10)
C(133)	4111 (5)	−474 (3)	5880 (3)	264 (12)
C(134)	5129 (5)	−824 (3)	6346 (3)	305 (12)
C(135)	5217 (5)	−1855 (3)	5879 (3)	300 (12)
C(136)	4286 (4)	−2504 (3)	4983 (3)	275 (12)
N(21)	256 (3)	−3583 (2)	1963 (2)	229 (9)
N(22)	−686 (3)	−3169 (2)	1556 (2)	226 (8)
N(24)	−1410 (3)	−4923 (2)	705 (2)	230 (9)
C(23)	−1661 (4)	−3987 (3)	810 (3)	210 (10)
C(25)	−210 (4)	−4623 (3)	1443 (3)	208 (10)
N(251)	1683 (3)	−4654 (2)	2624 (2)	225 (8)
C(252)	599 (4)	−5244 (3)	1789 (3)	208 (10)
C(253)	276 (5)	−6325 (3)	1349 (3)	279 (12)
C(254)	1052 (5)	−6848 (3)	1752 (4)	329 (13)
C(255)	2127 (5)	−6273 (3)	2595 (4)	351 (14)
C(256)	2412 (5)	−5184 (3)	3006 (3)	327 (14)
N(231)	−2839 (3)	−2677 (2)	718 (2)	226 (8)
C(232)	−2830 (4)	−3717 (3)	287 (3)	200 (10)
C(233)	−3844 (4)	−4431 (3)	−561 (3)	252 (12)
C(234)	−4929 (5)	−4102 (3)	−991 (3)	294 (12)
C(235)	−4976 (5)	−3067 (4)	−539 (3)	337 (13)
C(236)	−3920 (4)	−2375 (3)	301 (3)	285 (12)
O(11)	571 (3)	−1346 (2)	770 (2)	334 (8)
O(12)	2605 (3)	−1453 (2)	−308 (2)	399 (9)
O(13)	3216 (3)	−1166 (2)	1452 (2)	422 (9)
O(14)	−3044 (4)	−1965 (3)	3321 (3)	380 (10)
O(21)	−591 (3)	−3747 (2)	4107 (2)	476 (10)
O(22)	−2832 (3)	−3679 (2)	5018 (2)	534 (10)
O(23)	−3127 (4)	−3995 (2)	3248 (2)	626 (12)*
O(24)	3850 (5)	−2699 (3)	2251 (3)	394 (11)
S(1)	2214 (1)	−1066 (1)	703 (1)	270 (3)
S(2)	−2250 (1)	−4065 (1)	4062 (1)	333 (3)
C(1)	2643 (5)	362 (3)	1070 (3)	331 (13)
C(2)	−2668 (5)	−5474 (3)	3719 (4)	408 (15)
F(11)	1823 (3)	594 (2)	434 (2)	561 (9)
F(12)	2268 (3)	859 (2)	1988 (2)	454 (8)
F(13)	4115 (3)	767 (2)	1085 (2)	643 (10)
F(21)	−1944 (4)	−5697 (2)	4394 (3)	753 (12)
F(22)	−2253 (4)	−5984 (2)	2831 (2)	718 (11)
F(23)	−4156 (3)	−5886 (2)	3669 (3)	772 (12)*

[a] Estimated standard deviations in the least significant digits are given in parentheses. Atoms marked with an asterisk show high thermal anisotropy.

0.709 30 Å). Three standard reflections were measured periodically every 90 min, but no systematic loss of intensity was observed. The significant reflections ($I > 2\sigma(I)$) were not corrected for absorption. The intensities were corrected for Lorentz and polarization effects. Atomic scattering factors were taken from the literature.[20] Details on crystal data and intensity collection are listed in Table II.

Solution and Refinement of the Structure. The structure was solved by direct methods with the program MULTAN-78.[21] All following least-squares refinements and Fourier syntheses were based on the 2832 significant reflections. The function minimized was $\sum[w(|F_o| - |F_c|)^2]$ with $w = 1/\sigma_F^2$ ($\sigma_F^2 = \sigma_F^2$(counting statistics) + $0.014F^2$).

All hydrogen atoms were located in difference Fourier maps and were refined with isotropic temperature factors. All non-hydrogen atoms wer given anisotropic temperature factors in the refinement. The final values of the discrepancy indices, defined by $R = \sum(|F_o| - |F_c|)/\sum|F_o|$ and $R_w = [\sum w(|F_o| - |F_c|)^2/\sum w|F_o|^2]^{1/2}$ were $R = 0.0238$ and $R_w = 0.0278$ for the significant reflections while $R = 0.0451$ and $R_w = 0.0468$ for all data. No extinction correction was needed.

Atomic positions of the atoms are listed in Table III. Listings of F_o and F_c values, hydrogen atom parameters, anisotropic thermal parameters for the non-hydrogen atoms, and further bond distances and angles are available as supplementary material.[22]

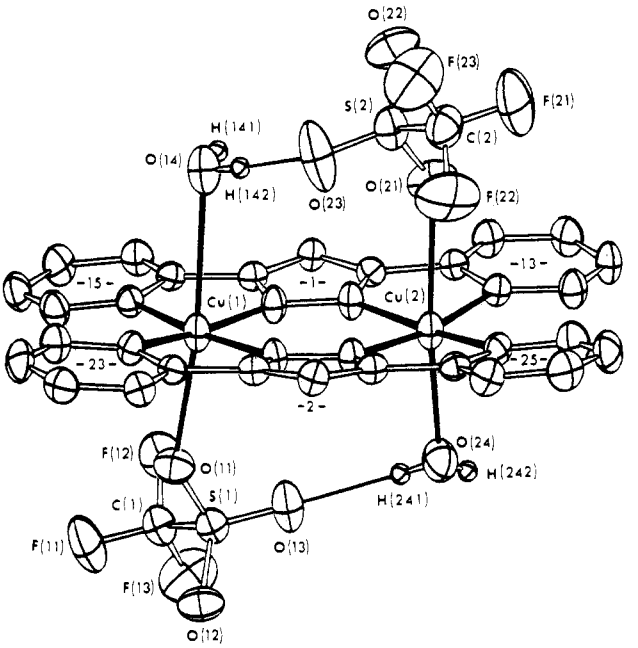

Figure 2. Projection of the structure of the dimeric unit $[Cu(bpt)(CF_3SO_3)(H_2O)]_2$ (**1**). Ligand ring indices correspond to the first (for triazole rings) and the first two (for the pyridine ring atoms) indices of the atomic parameters. Pyridine hydrogen atoms are omitted for clarity. Intramolecular hydrogen bonding is drawn as a thin line.

Table IV. Selected Bond Distances (Å)

Cu(1)–Cu(2)	4.085 (1)	N(14)–C(13)	1.347 (4)
Cu(1)–N(11)	1.942 (3)	N(14)–C(15)	1.343 (4)
Cu(1)–N(22)	1.936 (3)	C(13)–C(132)	1.464 (5)
Cu(1)–N(151)	2.082 (3)	C(15)–C(152)	1.462 (5)
Cu(1)–N(231)	2.087 (3)	N(21)–N(22)	1.348 (4)
Cu(1)–O(11)	2.376 (3)	N(21)–C(25)	1.326 (4)
Cu(1)–O(14)	2.802 (4)	N(22)–C(23)	1.333 (4)
Cu(2)–N(12)	1.950 (3)	N(24)–C(23)	1.340 (4)
Cu(2)–N(21)	1.932 (3)	N(24)–C(25)	1.344 (4)
Cu(2)–N(131)	2.090 (3)	C(23)–C(232)	1.453 (5)
Cu(2)–N(251)	2.090 (3)	C(25)–C(252)	1.452 (5)
Cu(2)–O(21)	2.799 (3)	O(14)–H(141)	0.73 (5)
Cu(2)–O(24)	2.323 (4)	O(14)–H(142)	0.86 (5)
N(11)–N(12)	1.348 (4)	O(24)–H(241)	0.79 (5)
N(11)–C(15)	1.330 (4)	O(24)–H(242)	0.74 (4)
N(12)–C(13)	1.314 (4)		

Results and Discussion

Description of the Structure of 1. A projection of the dimeric species is shown in Figure 2, together with the atomic labeling system used. Relevant bond lengths and angles are listed in Tables IV and V. The structure consists of dinuclear $[Cu(bpt)(CF_3SO_3)(H_2O)]_2$ molecules in which the copper centers appear at crystallographic inequivalent positions. The lack of a symmetry center between the copper atoms is reflected in the relatively small differences between the two copper chromophores in one dimeric

(20) "International Tables for X-ray Crystallography"; Kynoch Press: Birmingham, England, 1974; Vol. IV.
(21) Main, P.; Hull, S. E.; Lessinger, L.; Germain, G.; Declercq, J. P.; Woolfson, M. M. "A System of Computer Programs for the Automatic Solution of Crystal Structures from X-ray Diffraction Data"; Universities of York, England, and Louvain, Belgium, 1978.
(22) Supplementary material.

Table V. Selected Bond Angles (deg)

N(22)–Cu(1)–N(231)	79.3 (1)	Cu(2)–N(21)–N(22)	135.2 (2)
N(11)–Cu(1)–N(22)	90.2 (1)	Cu(2)–N(131)–C(136)	129.1 (2)
N(151)–Cu(1)–N(231)	111.3 (1)	Cu(2)–N(251)–C(256)	130.6 (3)
N(11)–Cu(1)–N(151)	79.1 (1)	N(12)–N(11)–C(15)	106.0 (3)
N(11)–Cu(1)–O(11)	100.1 (1)	N(11)–N(12)–C(13)	106.0 (3)
N(22)–Cu(1)–O(11)	95.4 (1)	N(12)–C(13)–N(14)	113.9 (3)
N(151)–Cu(1)–O(11)	86.4 (1)	N(14)–C(13)–C(132)	131.0 (3)
N(231)–Cu(1)–O(11)	90.3 (1)	N(12)–C(13)–C(132)	115.1 (3)
N(11)–Cu(1)–O(14)	80.7 (1)	C(13)–N(14)–C(15)	101.0 (3)
N(22)–Cu(1)–O(14)	93.8 (1)	N(11)–C(15)–N(14)	113.1 (3)
N(151)–Cu(1)–O(14)	84.7 (1)	N(11)–C(15)–C(152)	114.6 (3)
N(231)–Cu(1)–O(14)	90.6 (1)	N(14)–C(15)–C(152)	132.3 (3)
Cu(1)–N(11)–N(12)	134.8 (2)	C(13)–C(132)–C(133)	124.9 (4)
Cu(1)–N(22)–N(21)	134.9 (2)	C(13)–C(132)–N(131)	113.2 (2)
Cu(1)–N(151)–C(156)	129.7 (3)	C(15)–C(152)–C(153)	124.2 (4)
Cu(1)–N(231)–N(236)	129.7 (3)	C(15)–C(152)–N(151)	113.7 (3)
N(131)–Cu(2)–N(251)	111.1 (1)	N(22)–N(21)–C(25)	105.8 (3)
N(12)–Cu(2)–N(131)	78.6 (1)	N(21)–N(22)–C(23)	106.1 (3)
N(21)–Cu(2)–N(251)	79.5 (1)	N(22)–C(23)–N(24)	113.2 (3)
N(12)–Cu(2)–N(21)	90.1 (1)	N(22)–C(23)–C(232)	115.2 (3)
N(21)–Cu(2)–O(21)	85.9 (1)	N(24)–C(23)–C(232)	131.6 (4)
N(12)–Cu(2)–O(21)	93.3 (1)	C(23)–N(24)–C(25)	101.5 (4)
N(251)–Cu(2)–O(21)	77.1 (1)	N(21)–C(25)–N(24)	113.6 (3)
N(131)–Cu(2)–O(21)	91.2 (1)	N(24)–C(25)–C(252)	130.9 (3)
N(21)–Cu(2)–O(24)	93.1 (1)	N(21)–C(25)–C(252)	115.4 (3)
N(12)–Cu(2)–O(24)	95.1 (1)	C(23)–C(232)–N(231)	113.5 (3)
N(251)–Cu(2)–O(24)	94.5 (1)	C(23)–C(232)–C(233)	124.2 (3)
N(131)–Cu(2)–O(24)	91.4 (1)	C(25)–C(252)–N(251)	113.9 (3)
Cu(2)–N(12)–N(11)	134.5 (2)	C(25)–C(252)–C(253)	123.8 (4)

molecule. Apart from the tetradentate coordination by the two ligands one of the copper sites is axially coordinated by a trifluoromethylsulfonato anion and a water molecule at significantly larger distance. The axial coordination of the other copper atom is also completed by a water molecule and an anion, but in this case with a relatively short copper to water and a long copper to trifluoromethanesulfonate distance. The geometry of the nitrogen donor atoms can best be described as distorted square planar. Both copper atoms are slightly above the least-squares planes through their coordinating nitrogen atoms at the same side of the molecule. The distance from these atoms to these planes are 0.09 Å for Cu(1) and 0.12 Å for Cu(2). The copper–copper distance in the dimer is 4.085 (1) Å.

The equatorial coordination consists of two deprotonated ligands in which the copper atoms are linked by two triazole nuclei via their N(1)–N(2) bridging mode. Four pyridine nitrogen atoms complete the equatorial coordination around the two copper ions.

Both halves of the dimeric complex molecule show different triazole (trz) and pyridine (py) nitrogen to copper distances and N(py)–Cu–N(py) and N(trz)–Cu–N(trz) angles (see Table V). These features have also been observed for a related nickel compound possessing comparable differences in these distances and angles.[15] This coordination geometry is imposed on the structure by the geometry of the ligand. The distances between opposite pyridyl hydrogen atoms is about equal to the calculated van der Waals contacts[23] (i.e. H(136)···H(256) = 2.19 (4) Å; H(236)···H(156) = 2.23 (4) Å). All four of the pyridyl groups appear to be twisted slightly with respect to the center rings, possibly due to steric hindrance between these H atoms. The above-described possibility of steric hindrance may explain why no similar structures were found with ligands like 3,6-bis(pyridin-2-yl)-pyridazine.[24,25]

The crystal structure is further stabilized by intramolecular and intermolecular hydrogen bonds. The two intramolecular O···O contacts are in the usual range[26] (i.e. O(14)···O(23) = 2.814 (4) Å; O(14)–H(142)···O(23) = 176 (6)° and O(13)···O(24) = 2.953 (5) Å; O(13)···H(241)–O(24) = 175 (6)°). The intermolecular hydrogen-bonding pattern consists of an intermediate O···O contact and a weak N···O contact. The O···O contact extends between O(14) and O(24)′ of a symmetry-related molecule generated by $-1 + x, y, z$ with O(14)···O(24)′ = 2.864 (5) Å and O(14)···H-(242)′–O(24)′ = 173 (6)°. The weak N···O contact involves N(14) and O(14)″ of a molecule generated by $-x, -y, 1 - z$ with N-(14)···O(14)″ = 3.134 (5) Å and N(14)···H(141)″–O(14)″ = 168 (5)°.

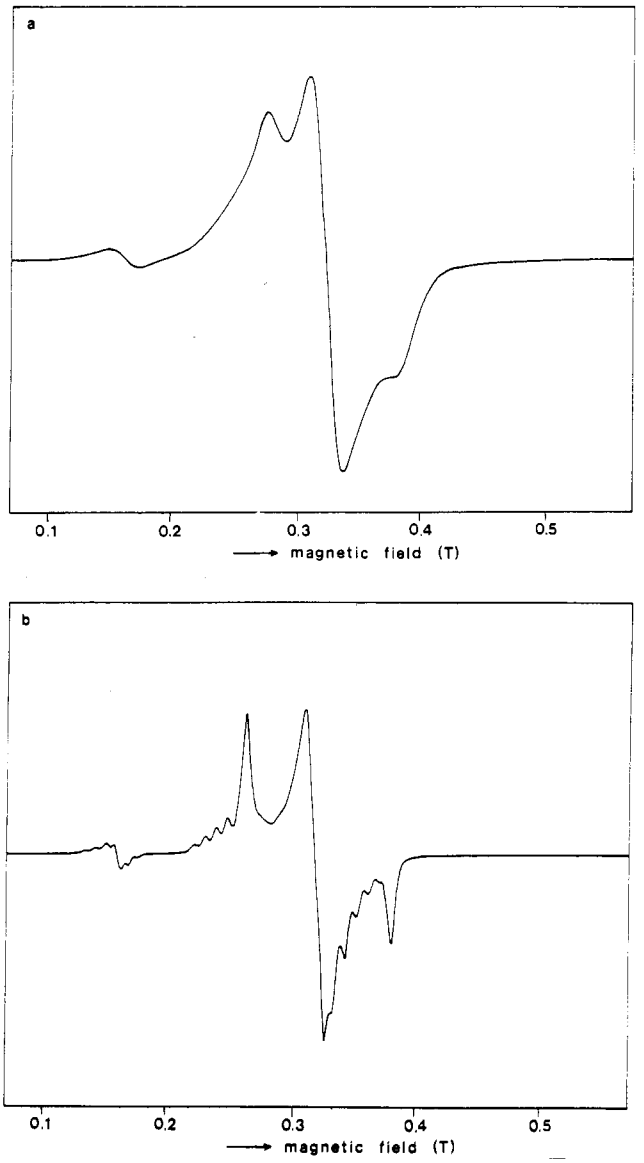

Figure 3. X-Band EPR spectra of $[Cu(bpt)(CF_3SO_3)(H_2O)]_2$ (**1**) at (a) room temperature (frequency 9.499 GHz) and (b) 77 K (frequency 9.204 GHz).

Electronic and EPR Spectra. The electronic spectra, which are also very much alike for all compounds mentioned in Table I, exhibit broad absorption maxima at about 16 000 cm^{-1} (see Table VI). Absorptions in this region are commonly observed for tetragonally distorted octahedral copper(II) complexes.[27,28] The frequently observed high-energy absorptions for copper(II) dimers[28,29] are present in the region 24 000–28 500 cm^{-1} as either distinguishable peaks or as a shoulder on a charge-transfer band.

The polycrystalline powder EPR spectra of the triflate compound at ambient temperature and 77 K are shown in Figure 3. The spectra are typical for copper dimers. Both $\Delta m_s = \pm 1$ and

(23) "Handbook of Chemistry and Physics"; CRC Press: Boca Raton, FL, 1979; Vol. 60.
(24) DeMunno, G.; Denti, G.; Dapporto, P. *Inorg. Chim. Acta* **1983**, *74*, 199.
(25) DeMunno, G.; Denti, G. *Acta Crystallogr., Sect. C: Cryst. Struct. Commun.* **1984**, *C40*, 616.
(26) Schuster, P., Zadel, G., Sandorfy, G., Eds. "The Hydrogen Bond", North-Holland: Amsterdam, 1978.
(27) Hathaway, B. J.; Billing, D. E. *Coord. Chem. Rev.* **1970**, *5*, 143.
(28) Reedijk, J.; Knetsch, D.; Nieuwenhuijse, B. *Inorg. Chim. Acta* **1971**, *5*, 568.
(29) Nonoyama, K.; Ojima, H.; Nonoyama, M. *Inorg. Chim. Acta* **1984**, *84*, 13.

Table VI. Spectroscopic and Magnetic Data of the Copper(II)–bpt Compounds[d]

compd	visible spectra band max, cm^{-1}	EPR data					magnetic data	
		g_x	g_y	g_z	D, cm^{-1}	E, cm^{-1}	J,[b] cm^{-1}	p,[a] %
1[c]	26 000 m, 16 000 br	2.08 (3)	2.04 (3)	2.19 (3)	0.06 (1)	0.02 (1)	−118 (10)	0
2	28 200 sh, 16 000 br	2.13 (3)	2.03 (3)	2.21 (3)	0.06 (1)	0.01 (1)	−113 (10)	1
3	27 700 sh, 16 000 br	2.12 (3)	2.05 (3)	2.20 (3)	0.07 (1)	0.02 (1)	−105 (10)	6
4	28 400 sh, 16 200 br	2.13 (3)	2.02 (3)	2.21 (3)	0.06 (1)	0.01 (1)	−102 (10)	3

[a] p stands for the fraction of paramagnetic impurity. [b] The used exchange Hamiltonian is defined in the text. [c] The spectrum of this compound reveals hyperfine splitting on the HZ absorptions of 9×10^{-3} T at 77 K. [d] Estimated standard deviations in the least significant digits are given in parentheses.

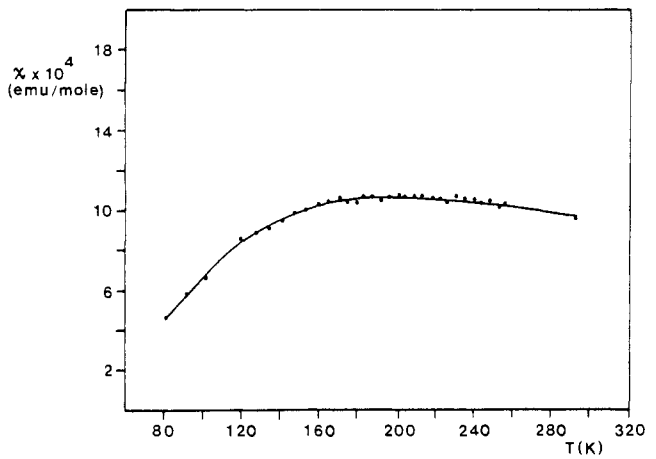

Figure 4. Plot of the magnetic susceptibility vs. temperature for $[Cu(bpt)(ClO_4)(H_2O)]_2(H_2O)_2$ (**2**). The solid line indicates the best fit to the theoretical susceptibility with parameters $g = 2.07$, $J = -113$ cm^{-1} and a 1% amount of paramagnetic impurity.

$\Delta m_s = \pm 2$ absorptions are clearly observed. The spectra exhibit a significant decrease in intensity of the absorptions upon cooling the sample from room temperature to 77 K. This results from depopulation of the triplet state.[30,31]

The spectra of the triflate compound as shown in Figure 3 are the most remarkable as they show copper hyperfine interactions superimposed on the HZ absorptions with a value of $A = 9.0$ mT in the 77 K spectrum. This is a feature that is seldom observed for magnetically undiluted copper(II) powders. In this case the appearance of the hyperfine splitting results from the presence of quite isolated spin triplet states in the sample and is probably caused by the large interdimer distance. The other three compounds, which contain somewhat smaller anions, may have smaller interdimer distances and consequently do not show this hyperfine splitting. The triflate compound is described in more detail by means of single-crystal EPR measurements in a later study.[31]

Magnetic Measurements. To obtain detailed information about the singlet–triplet splittings in the compounds, magnetic susceptibilities were determined as a function of temperature. The magnetic susceptibility of $[Cu(bpt)(CF_3SO_3)(H_2O)]_2$ in the 80–300 K region is shown in Figure 4.

Considering only nearest-neighbor interactions, the exchange Hamiltonian for dinuclear species is usually expressed as $H_{ex} = -2J[\hat{S}_1 \cdot \hat{S}_2]$. For copper(II) compounds this Hamiltonian defines the energy gap between the singlet and triplet states as $2J$. The theoretical expression for the magnetic susceptibility as a function of T is the well-known Bleaney-Bowers equation.[32] The formula

$$\chi_a = \frac{Ng^2\beta^2}{kT}[3 + \exp(-2J/kT)]^{-1}(1 - p) + \chi_{TIP} + p\frac{Ng^2\beta^2 S(S+1)}{kT}$$

in which the symbols have their usual meaning, gives the magnetic susceptibility per mole of copper atoms in the coupled system, corrected for TIP and paramagnetic impurities. The temperature-independent paramagnetism χ_{TIP} was taken as 60×10^{-6} emu/mol. The third term in the equation takes account of the fraction of paramagnetic impurity. Experimental data, which were corrected for diamagnetism, were fitted to this equation by means of a least-squares procedure, having J and the average g value as fitting parameters. The best values are listed in Table VI. As could be expected from the EPR data and the planarity of dimer molecules, the fits yield values for the exchange constant J in the range −102 to −118 cm^{-1}. Comparison of the J values as listed in Table VI shows that they are all very similar. Considering the large copper–copper distance in the dimer, a superexchange pathway must be responsible for the strong antiferromagnetic interaction. Although the Cu–N(trz)–N(trz) and the Cu–N(py)–N(py) angles deviate considerably from the ideal values resulting in maximum deviate considerably from the ideal values resulting in maximum overlap density, the magnitude of the J values nevertheless indicates that there is a considerable amount of interaction via the ligand molecular orbitals and that the magnetic orbitals of the copper atoms are in the same plane. Considering recent investigations, it is suggested that the exchange is mainly determined by a σ overlap superexchange pathway[33,34] involving σ electrons of the heterocycle.[4] Quantitative discussions on the correlation between exchange and geometric parameters will not be given, because they can only be made when a series of structurally comparable compounds with related ligands having different bonding properties is investigated.

Concluding Remarks

The results described in this paper indicate that 3,5-disubstituted 1,2,4-triazoles, which can act as tetradentate ligands, are very suitable for studying exchange-coupled pairs of transition-metal ions.

The planarity of the ligand, which imposes a planar structure on the coordination compounds, allows an extension of the already available magnetic data on tetragonal compounds. The tetragonally coordinated copper(II) compounds are compounds whose magnetic properties have been investigated very thoroughly over the past two decades. Although as a result of this the magnetism of such compounds is reasonably well understood, detailed conclusions on structural–magnetic correlations cannot be drawn until more data are available on such triazole-bridged systems.

Another interesting aspect of these ligands is the irregular geometry they induce, resulting in low-symmetry coordination geometries around metal ions, which can be studied with the aid of ligand field spectroscopy. Spectroscopic indications for this low symmetry are not so strong for Cu(II) but are likely to be much more pronounced in the case of Ni(II) and Co(II), which are more accessible to spectroscopic studies. Studies about these spectroscopic properties of compounds with bpt and related ligands are in progress.

Forthcoming investigations will deal with related ligands to allow a more detailed study of structural–magnetic correlations.

Acknowledgment. We wish to express our gratitude to S. Gorter

(30) Bencini, A.; Benelli, C.; Gatteschi, D.; Zanchini, C.; Fabretti, A. C.; Francini, G. C. *Inorg. Chim. Acta* **1984**, *86*, 1694.
(31) Bencini, A.; Gatteschi, D.; Zanchini, C.; Haasnoot, J. G.; Prins, R.; Reedijk, J. *Inorg. Chem.* **1985**, *24*, 2812.
(32) Bleaney, B.; Bowers, K. D. *Proc. R. Soc. London, Ser. A* **1952**, *214*, 451.
(33) Kahn, O. *Inorg. Chim. Acta* **1982**, *62*, 3.
(34) Haddad, M. S.; Wilson, S. R.; Hodgson, D. J.; Hendrickson, D. N. *J. Am. Chem. Soc.* **1981**, *103*, 384.

and R. C. M. de Groot for their assistance with X-ray data collection and magnetic measurements, respectively.

Registry No. **1**, 98758-75-9; **2**, 98720-88-8; **3**, 98759-90-1; **4**, 98720-89-9.

Supplementary Material Available: Listings of observed and calculated structure factors, fractional atomic coordinates and isotropic thermal parameters for the hydrogen atoms, anisotropic thermal parameters for the non-hydrogen atoms, and further bond distances and angles (15 pages). Ordering information is given on any current masthead page.

Contribution from the Laboratoire de Physico-Chimie Moléculaire, UA 474, Institut Universitaire de Recherche Scientifique, 64000 Pau, France, and Laboratoire CNRS-SNPE, 94320 Thiais, France

Stabilization of Phosphinidene and Phosphirene by Complexation on Phosphorus. Theoretical Studies and Photoelectron Spectra†

D. GONBEAU,‡ G. PFISTER-GUILLOUZO,*‡ A. MARINETTI,§ and F. MATHEY§

Received December 7, 1984

Electronic structures of phosphinidene and phosphirene complexes are described, extended Hückel theory, ab initio calculations, and data from UV photoelectron spectroscopy in conjunction. The nature of the metal–phosphorus double bond in these compounds was investigated. The stabilization of phosphinidene and phosphirene by complexation on phosphorus was studied on the basis of the diagram of orbital correlation with the fragment orbitals. These conclusions agree with analysis of photoelectron spectra of stable phosphirene complexes.

The chemistry of phosphinidene complexes has been extensively studied by two of us.[2] A similarity between the behavior of terminal complexes of phosphinidene and that of singlet carbene was suggested.

The present report is a quantum-chemical examination of this entity. The nature and the electronic origin of the M–P bonds (M = Cr, Fe) were first analyzed on the basis of a diagram of orbital interactions between the different orbitals of the fragments, obtained from extended Hückel theory (EHT) calculations. This method, previously used with success for the study of Fischer type carbene complexes[3] of Schrock complexes,[4] does not lead to a rigorous determination of spin states. For this reason, we carried out a more sophisticated PSHONDO ab initio calculation[5] on pentacarbonyl(phosphinidene)chromium. Various results[6] have shown that this formalism generates results comparable to those of "all electrons" SCF calculations.

In parallel to the data it supplied on the electronic structure of complexed phosphinidene, this approach was used as the basis for studying the system of complexed phosphirene, the only stable compound isolated. The photoelectron spectra of a number of derivatives of the latter compound were analyzed in order to utilize these experimental data to verify the coherency of conclusions drawn from the quantum-chemical study.

Computational and Experimental Details

EHT calculations were performed with the parameters previously utilized[4] for Cr and Fe.

All SCF calculations were carried out with use of version of the HONDO program PSHONDO.

For carbon, oxygen, and phosphorus the pseudopotentials and basis sets chosen were those previously determined.[7] The four Gaussian functions were contracted to the double-ζ level (3 + 1) for each atom except for carbon and oxygen in $Cr(CO)_5$, which were treated at the single-ζ level, because of the considerable computing effort in the case of the phosphirene complex. For phosphorus, a 3d Gaussian was added (α_d = 0.57) as a polarization function.

We have determined the nonempirical atomic pseudopotential for chromium from the atomic Hartree–Fock calculations of Clementi and Roetti.[8] A valence basis set (4s,4p,3d) was optimized for this atom in a pseudopotential SCF calculation of the atomic ground state, with use of a basis set previously proposed.[9] For 4s and 3d orbitals these Gaussian functions were contracted to the double-ζ level by means of a 2 + 1 procedure for 4s and 4 + 1 for 3d.

The Gaussian valence basis set and pseudopotentials are described in Tables I and II.[10]

The SCF valence energies for the open-shell triplet states were obtained by calculating the mean value of the H operator between the wave functions, determined from a Nesbet type operator.[11]

According to Koopmans' theorem (KT) the monoelectronic levels are related to ionization potentials (IP's). However, KT IP's do not take into account polarization and correlation effects. The following procedure[12] was used to estimate the corrections (to KT values) required to reach more realistic IP's. Polarization of the positive ion is approximated by first-order perturbation theory as

$$\Delta\epsilon_k(\text{pol}) = \sum_{ij^*} \frac{\langle i|F_k^+|j^*\rangle^2}{\epsilon_i - \epsilon_{j^*}}$$

where F_k^+ is the Fock operator obtained after removal of one electron from orbital k and i and j^* are the SCF molecular orbitals of the neutral molecule. The main part of correlation decrease in the positive ion is due to the lack of double excitations from orbital k and can be approximated by

$$\Delta\epsilon_k(\text{cor}) = \sum_{j^*l^*} \frac{\langle kj^*|kl^*\rangle^2}{2\epsilon_k - \epsilon_{j^*} - \epsilon_{l^*}}$$

Both contributions are easy to evaluate and require a computing effort equivalent to only one SCF iteration.

† Application of Photoelectron Spectroscopy to Molecular Properties. 25. For Part 24, see ref 1.

‡ Institut Universitaire de Recherche Scientifique.

§ Laboratoire CNRS–SNPE.

(1) Part 24: Garcia, J. L.; Gonbeau, D.; Pfister-Guillouzo, G.; Roch, M.; Weber, J. *Can. J. Chem.*, in press.
(2) (a) Marinetti, A.; Mathey, F.; Fischer, J.; Mitschler, A. *J. Chem. Soc., Chem. Commun.* **1982**, 667 (b) Marinetti, A.; Mathey, F.; Fischer, J.; Mitschler, A. *J. Am. Chem. Soc.* **1982**, *104*, 4484 (c) Marinetti, A.; Mathey, F. Organometallics, **1984**, *3*, 456.
(3) Hoffmann, R. *Angew. Chem., Int. Ed. Engl.* **1982**, *21*, 711 and references cited therein.
(4) Goddard, R. J.; Hoffmann, R.; Jemmis, E. D. *J. Am. Chem. Soc.* **1980**, *102*, 7667.
(5) (a) Dupuis, M.; Rys, J.; King, H. F. *J. Chem. Phys.* **1976**, *65*, 111. (b) Durand, P.; Barthelat, J. C. *Theor. Chim. Acta* **1975**, *38*, 283.
(6) (a) Barthelat, J. C.; Durand, P. *Gazz. Chim. Ital.* **1978**, *108*, 225. (b) Dixon, R. N.; Robertson, I. L. *Theor. Chem. (London)* **1978**, *3*, 100.
(7) Laboratoire de Physique Quantique, Toulouse Ateliers, France (October 1981).
(8) Clementi, E.; Roetti, C. *At. Data Nucl. Data Tables* **1974**, *14*, 177.
(9) (a) Wachters, A. J. H. *J. Chem. Phys.* **1970**, *52*, 1033. (b) Rappe, A. K.; Smedley, T. A.; Goddard, W. A. *J. Chem. Phys.* **1981**, *85*, 2607.
(10) Supplementary material.
(11) Nesbet, R. K. *Rev. Mod. Phys.* **1963**, *35*, 552.
(12) (a) Malrieu, J. P. *J. Spectrosc. Photoélectronique* **1978**. (b) Trinquier, G. *J. Am. Chem. Soc.* **1983**, *104*, 6969. (c) Gonbeau, D.; Pfister-Guillouzo, G. *J. Electron. Spectrosc. Relat. Phenom.* **1984**, *33*, 279.

0020-1669/85/1324-4133$01.50/0